Control of Microstructures and Properties of a Phosphorus-Containing Cu-0.6 Wt.% Cr Alloy through Precipitation Treatment

N. Gao, T. Tiainen, Y. Ji, and L. Laakso

(Submitted 17 July 2000)

A phosphorus-containing Cu-0.6 wt.% Cr alloy was solution treated and then aged using various combinations of time and temperature. The influence of aging time and temperature on microstructures and properties of this alloy was investigated by means of an analytical transmission electronic microscope (TEM) and measurements of hardness and electrical conductivity. It was found that neither underaging nor overaging could harden the alloy significantly. The microstructure corresponding to peak hardness was characterized by very fine and coherent precipitates. Increasing aging time and temperature caused the precipitates to grow into rodlike incoherent Cr particles having body-centered cubic (bcc) crystal structure, but aging temperature influenced the microstructures and properties more intensively than did aging time. Undissolved body-centered tetragonal (bct) Cr_3P particles, which were found in both as-solution-treated and as-aged structures, were not harmful to electrical conductivity and might act as obstacles impeding dislocation motion. As compared to a Cu-0.65 wt.% Cr alloy not containing phosphorus, the studied alloy needs aging at a higher temperature to reach peak hardness.

Keywords copper-chromium alloy, electron microscopy, hardness, heat treatment, precipitation hardening

1. Introduction

Precipitation-hardenable copper-chromium alloys containing 0.6 to 1.2 wt.% Cr have so far received much attention because of their excellent combination of high strength and high electrical conductivity. The influence of processing parameters on the microstructures and properties of copper-chromium alloys has been intensively studied.[1–9] These alloys are usually solution treated for 30 to 60 min at temperatures ranging from 950 to 1020 °C, and subsequently aged at temperatures ranging from 400 to 600 °C. Solution treatment at 1000 °C for 60 min is considered as practical processing for industrial use. During the aging treatment, very fine and coherent Cr-rich precipitates appear in the early stage and they grow and coarsen into incoherent body-centered cubic (bcc) Cr precipitates with increasing time or temperature.

In contrast to the conventional copper-chromium alloys mentioned above, copper-chromium alloys containing trace amounts of phosphorus have received little attention. So far, phosphorus in copper-chromium alloys has been regarded only as an impurity. Witcomb *et al.*[10] found that bct Cr_3P coprecipitated with the primary Cr precipitate laths in a Cu-Cr alloy containing 0.012 wt.% phosphorus impurity. Using the same alloy, Luo *et al.*[11] further investigated the effect of phosphorus on the growth of precipitates as well as on the orientation relationship between the precipitate and the matrix. However, the two studies did not involve the effect of phosphorus impurity on the properties of the Cu-Cr alloy. Moreover, the influence of a relatively high addition of phosphorus on structures and properties of a Cu-Cr alloy still remains unknown. Thus, the present work focuses on a Cu-0.6 wt.% Cr alloy containing more than 0.06 wt.% phosphorus (Cu-0.6Cr-0.07P alloy). After solution treatment, the alloy is aged using various combinations of time and temperature. The influence of aging time and temperature on properties and microstructures of the alloy is studied and a comparison is made between the alloy and a Cu-0.65 wt.% Cr alloy not containing phosphorus.

2. Experimental

Ingots of the alloy were prepared from highly pure elements by vacuum casting. Table 1 presents the composition in weight percentage. After homogenization treatment at 1050 °C for 30 min, the ingots were hot extruded into rods of about 16 mm diameter.

Specimens were separately solution treated for 60 min at 980 and 1000 °C, and for 30 min at 1020 °C, after which they were quickly quenched into water. The solution-treated specimens were aged at the temperatures of interest for times ranging from 30 to 240 min. Hardness measurements were carried out using a Zwick

Table 1 Composition of the studied alloy (wt.%)

Cu	Cr	P	Impurities
Remainder	0.61	0.068	<0.02

N. Gao, T. Tiainen, and **Y. Ji**, Tampere University of Technology, Institute of Materials Science, Tampere 33101, Finland. **L. Laakso**, Outokumpu Poricopper R&D, Pori 28101, Finland. Contact e-mail: gao.nan@tut.fi.

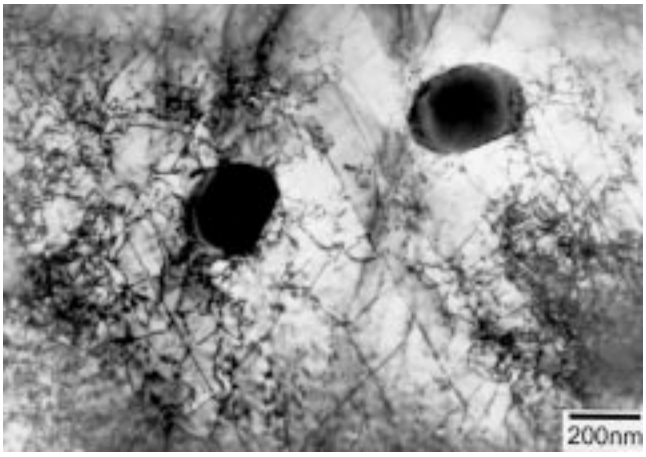

(a)

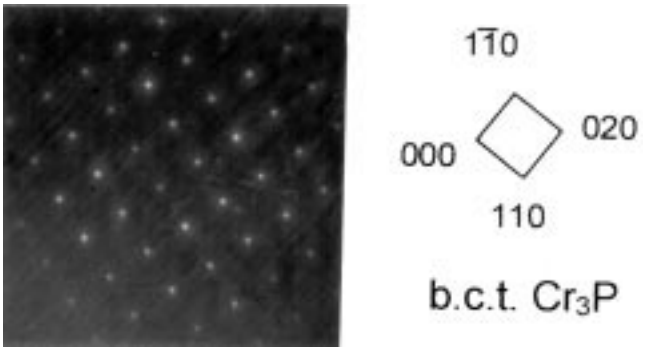

(b)

Fig. 1 TEM micrographs of the solution-treated Cu-0.6Cr-0.07P alloy. (**a**) Undissolved particles with dislocations. (**b**) SADP from one of the undissolved particles and its identification

hardness tester (Zwick GmbH & Co., Ulm, Germany) with 3 kg load. The electrical conductivity of aged specimens was measured using a Sigmatest (Foerster Ltd., U.K.) apparatus. A JEOL JEM-2010 analytical transmission electron microscope (TEM) with an acceleration voltage of 200 kV (Japan Electron Optics Ltd., Tokyo) was employed for microstructural studies. Thin disks cut from the heat-treated specimens were ground and then thinned into TEM films by the window method in a solution containing 1 part nitric acid and 2 parts methanol at a temperature below −40 °C.

3. Results and Discussion

3.1 Solution-Treated Specimens

Figure 1(a) shows the solution-treated microstructure of the alloy, where two particles are surrounded by dislocations. Quick quenching from a high solution-treating temperature (*e.g.*, 1000 °C) produced a high density of dislocations at the particle-matrix interface. These egg-shaped particles were not formed by precipitation during quenching but most possibly formed during the solidification of the alloy because of their large size. The result of energy dispersive spectroscopic analysis revealed that the particles contained both Cr and P. The selected area diffraction pattern (SADP) (Fig. 1b) recorded from one of the particles was identified as the pattern of [001] zone axis of Cr_3P having a body-centered tetragonal (bct) crystal structure. No orientation relationship was found between the Cr_3P particles and the matrix.

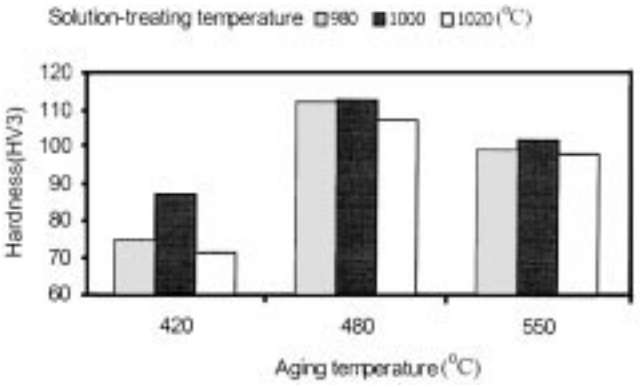

Fig. 2 Effect of solution-treating temperature on hardness of Cu-0.6Cr-0.07P alloy after aging

Figure 2 compares the hardness values measured from the specimens aged at 420, 480, and 550 °C. Clearly, aging either at 420 °C or at 550 °C resulted in a lower hardness than did aging at 480 °C. Thus, aging at 420 °C might result in an underaged structure and aging at 550 °C an overaged structure. Neither underaging nor overaging could produce a maximal hardening effect, even though the alloy had been solution treated at different temperatures before aging. Figure 2 also suggests that solution-treating temperature influences the alloy hardness after aging. The solution treatment at 1000 °C caused the alloy to gain more hardness by subsequent aging than did other solution treatments. As used for copper-chromium alloys not containing phosphorus, therefore, solution treatment at 1000 °C is also a good processing for Cu-0.6Cr-0.07P alloy.

3.2 Aged Specimens

The microstructures of the alloy evolved as either aging time or aging temperature increased. Very fine and coherent precipitates were formed when the specimen was aged for 60 min at 510 °C, as shown in Fig. 3(a). With prolonged aging, the precipitates grew up into spherical particles (Fig. 3b). In contrast, the precipitates formed by aging for 60 min at 550 °C (Fig. 3c) had almost the same size as those formed by aging for 240 min at 510 °C. When aged under these two conditions, most of the precipitate particles showed no contrast lines in their middles. This feature arises from the coherent strain field caused by the difference between the lattice parameters of precipitate and matrix.[12] However, the large rodlike precipitate particles that were formed by aging at 700 °C (Fig. 3d) are clearly incoherent with the matrix.

The precipitate morphologies presented in Fig. 3 suggest that aging temperature had a stronger influence on precipitate growth than did aging time. The precipitate coarsening rate obeys the following equation,[13] which is derived on the assumption that coarsening is controlled by the diffusion of solute atoms in the matrix:

$$\bar{r}^3 - \bar{r}_0^3 = kt \qquad \text{(Eq 1)}$$

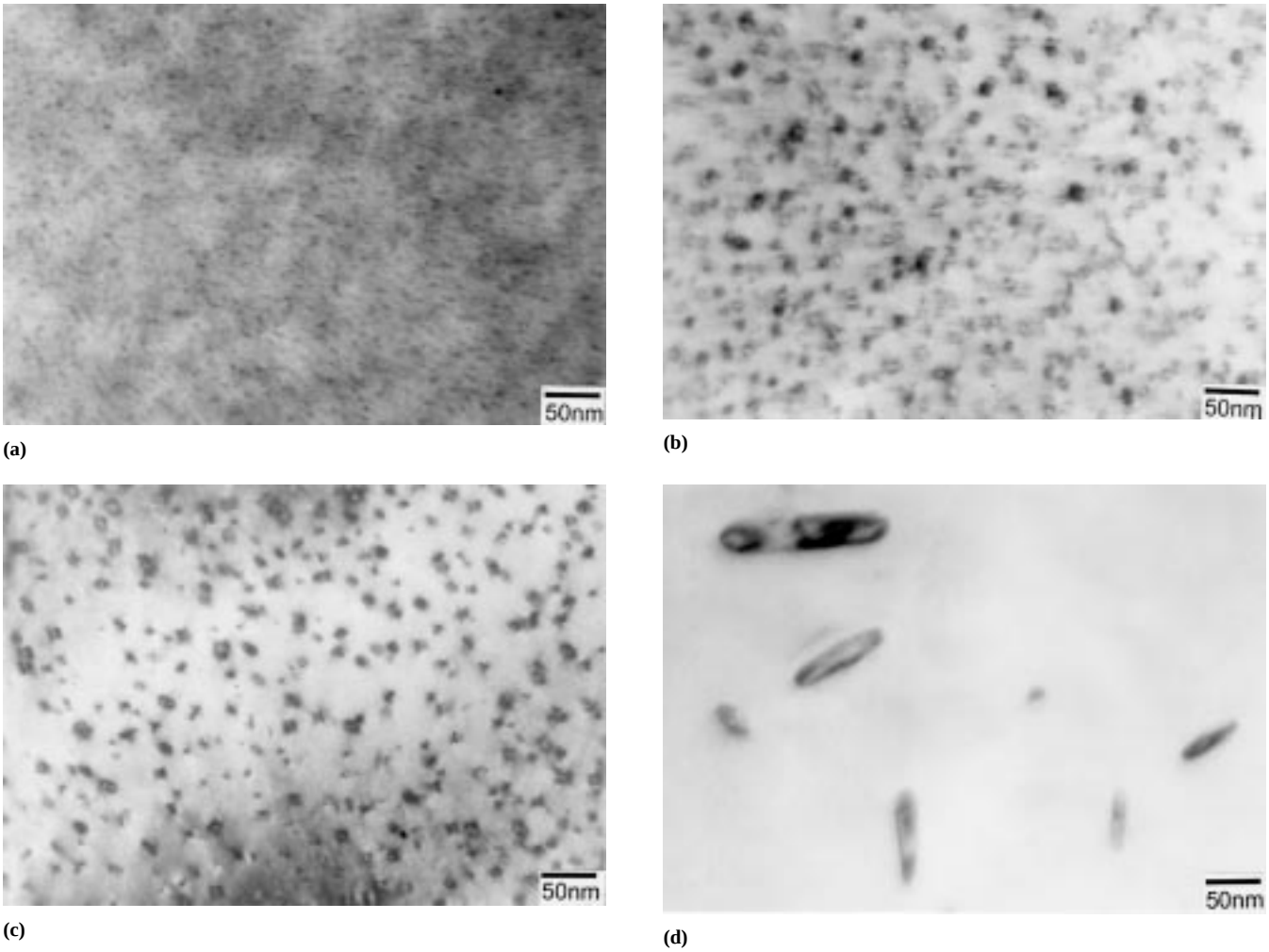

Fig. 3 TEM micrographs showing evolution of precipitate morphologies of Cu-0.6Cr-0.07P alloy after aged at (**a**) 510 °C for 60 min, (**b**) 510 °C for 240 min, (**c**) 550 °C for 60 min, and (**d**) 700 °C for 120 min

where $\bar{r}_0$ is the average precipitate particle radius at the onset of coarsening and k is a rate constant given by

$$k \propto D\gamma X_e \qquad \text{(Eq 2)}$$

where D is the diffusion coefficient for the solute diffusion in matrix, γ is the interfacial energy between precipitate and matrix, and X_e is the equilibrium solubility of the solutes in the matrix. As indicated by Eq 2, the value of k depends mainly on D and X_e. Since D increases exponentially with temperature, the rate of coarsening will also increase rapidly with temperature.

When the aging temperature was increased up to 700 °C, the precipitates coarsened dramatically and transformed into rodlike incoherent particles (Fig. 3d). Figure 4(a) shows a large rodlike precipitate particle that was formed by aging at 700 °C, and Fig. 4(b) is its dark-field image. The SADP from this particle was identified as the pattern of bcc Cr [001] zone axis (Fig. 4b). However, it is worth noting that only part of the precipitate particle appears bright under dark-field conditions. This may suggest that bcc Cr is not the only phase in the large precipitate particle formed by aging for 360 min at 700 °C.

Besides precipitates, another type of phase particles was found in as-aged structures. The TEM micrograph in Fig. 5(a) reveals the shape and size of the particles. Clearly, they are similar in shape to those in Fig. 1(a), but appear to be larger. Figure 5(c) is the SADP recorded from one of the particles in the structure aged for 60 min at 510 °C. It was identified as a complex pattern consisting of the patterns of bct Cr_3P with [001] and fcc Cu (matrix) with [$\bar{3}$32] zone axes. However, no definite orientation relationship was found between the Cr_3P phase and the matrix in the as-aged structure. Evidently, these large egg-shaped Cr_3P particles did not precipitate during aging treatment because they were much larger than the precipitate particles shown in Fig. 3(b). Thus, the Cr_3P particles in the as-aged structure would be the same type of particles seen in the as-solution-treated structure, but they became larger due to aging. Figure 5(b) shows an undissolved Cr_3P particle impeding the movement of a dislocation line. It suggests that the undissolved Cr_3P particles in the as-aged structures can impede dislocation motion, thereby playing a dispersion-strengthening role. However, they probably increased the alloy strength marginally due to their sparse distribution. The large interparticle spacing

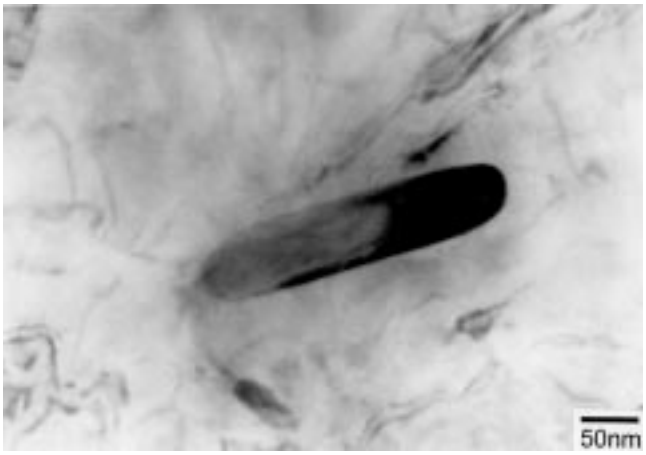

(a)

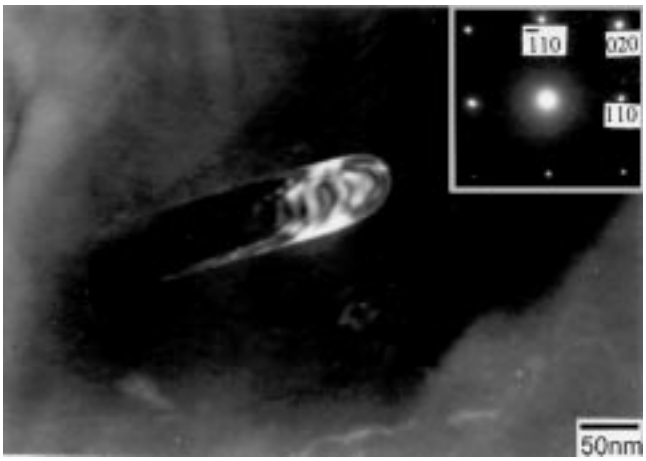

(b)

Fig. 4 A rodlike precipitate particle formed by aging for 360 min at 700 °C. (**a**) Bright-field TEM micrograph. (**b**) Dark-field TEM micrograph and its identified SADP (bcc Cr with [001] zone axis pattern)

between them weakens their role as obstacles to dislocation motion.[14]

The precipitate-free zones (PFZs) were observed in the vicinity of the grain boundary and of the Cr_3P particles in Figs. 5(a) and 6. As a stable incoherent phase, the undissolved Cr_3P particles grew with the dissolution of coherent precipitates surrounding them during aging. This is a reason for the presence of PFZs around the undissolved Cr_3P particles. The PFZ is also a consequence of the fact that quick quenching results in a large number of excess vacancies, which are ideal for the occurrence of homogenous nucleation. However, the quench-in vacancies having a high diffusivity easily sink in the vicinity of grain boundaries or interfaces.[13] Because of the lack of excess vacancies, the PFZ was formed in the areas adjacent to the grain boundary shown in Fig. 6.

The present work did not show the presence of Cr_3P precipitate but only bcc Cr phase. However, this does not mean that Cr_3P precipitates would not form in the studied alloy. As compared to the aging conditions (700 °C for 960 min and 863 °C

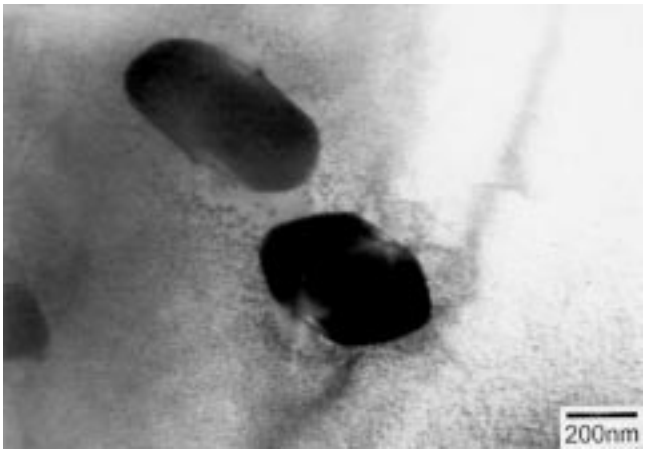

(a)

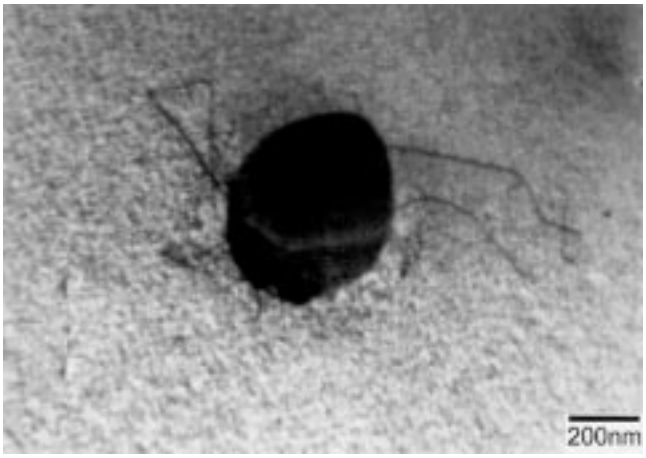

(b)

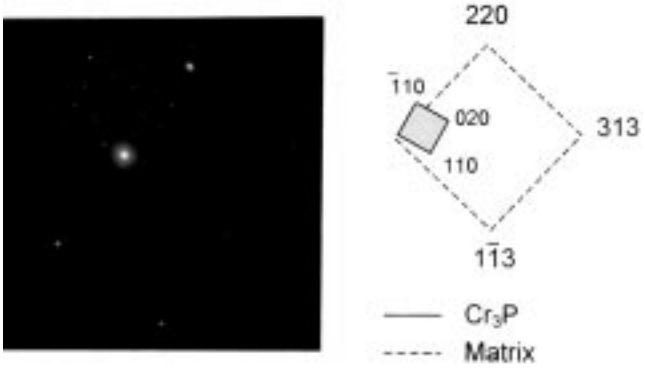

(c)

Fig. 5 TEM micrographs of undissolved Cr_3P particles in Cu-0.6Cr-0.07P alloy aged for 60 min at 510 °C. (**a**) Two undissolved particles with precipitate-free zones near them. (**b**) Interaction of an undissolved particle with a dislocation line. (**c**) SADP from (b) and its identification

for 1440 min) used in Ref 10 and 11, aging at 700 °C for 360 min was the severest aging treatment used in the present work. Since it has much higher phosphorus concentration than the alloy studied in Ref 10 and 11, the present alloy would most probably show not only primary Cr but also Cr_3P precipitates

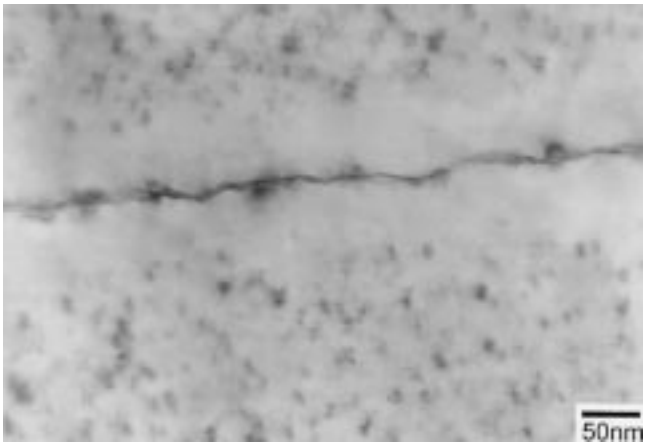

Fig. 6 TEM micrograph showing a precipitate-free zone in the vicinity of a grain boundary in Cu-0.6Cr-0.07P alloy aged for 240 min at 510 °C

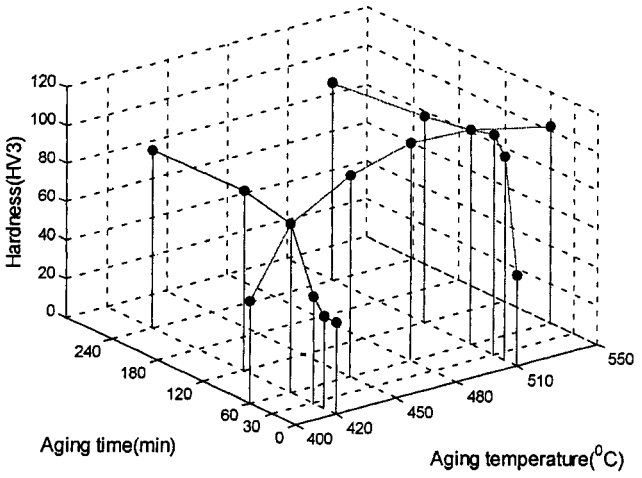

Fig. 7 Dependence of hardness of Cu-0.6Cr-0.07P alloy on aging time and aging temperature

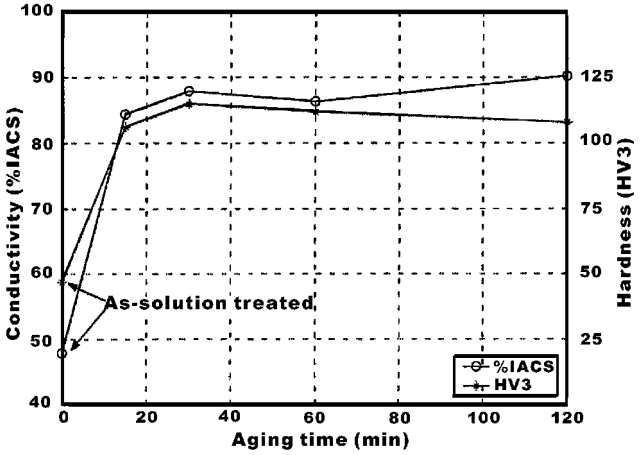

Fig. 8 Electrical conductivity and hardness of Cu-0.6Cr-0.07P alloy as a function of aging time (aging at 510 °C)

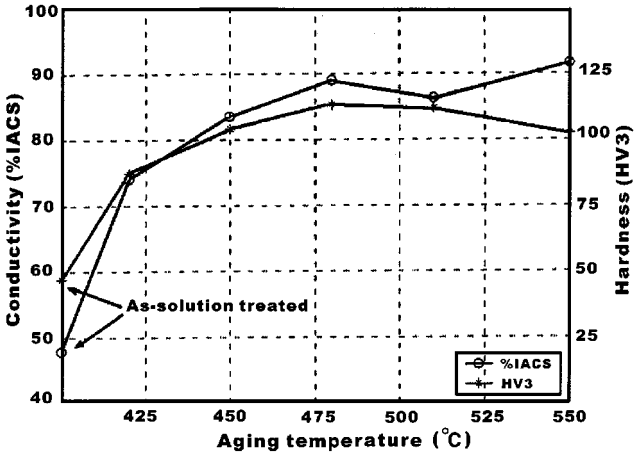

Fig. 9 Electrical conductivity and hardness of Cu-0.6Cr-0.07P alloy as a function of aging temperature (aging for 60 min)

with further increase in aging time and temperature. This suggestion is further supported by the fact that undissolved Cr_3P particles were found in the as-solution-treated structures. These particles were most probably formed either during solidification of the alloy or during solution treatment at a high temperature. Their high stability prevented their dissolution during aging.

Figure 7 shows the dependence of the alloy hardness on both aging time and temperature. The short-time aging at 420 °C resulted in relatively low hardness, but even the prolonged aging at this temperature resulted in only a marginal gain in hardness. In contrast, aging at 510 °C not only made the alloy hard sooner, but also made it much harder than did aging at 420 °C. Therefore, the general tendency by which the alloy hardness responds to aging treatment includes that the hardness reaches a maximum with increasing aging time and temperature, after which it will decrease when the alloy is overaged.

The alloy hardness is dependent on both aging time and aging temperature, and the latter influences the hardness more markedly. As discussed before, the microstructure of the alloy has the same dependence on aging time and temperature. This means that the hardness behavior of the alloy corresponds well to its microstructural evolution during aging. In the present work, no precipitates were seen in the specimens aged for less than 60 min at temperatures below 450 °C even at the high magnifications (up to 1,000,000×) of TEM. This does not rule out precipitation below 450 °C, but the small increase in hardness implies that the precipitates were still in the nucleation stage and their stress fields were not strong enough to resist dislocation motion. On the other hand, under overaging conditions, the precipitates grew and coarsened so that their distribution became sparse and the interparticle spacing wide. The increased interparticle spacing reduced the resistance to dislocation motion. Thus, the very fine and coherent precipitate morphology shown in Fig. 3(a) corresponded to a better strengthening effect than the coarsened precipitate morphologies in Fig. 3(d).

Figures 8 and 9 show the variations of conductivity and

hardness of the alloy under isothermal and isochronal aging conditions. The hardness and conductivity responded similarly to the two aging conditions, that is, aging at 510 °C for times less than 30 min or aging at temperatures below 480 °C for 60 min improves both hardness and conductivity significantly. However, neither the hardness nor the conductivity showed a continuous increase with aging time or temperature. As shown in Fig. 8, increasing aging time caused not only a significant increase, but also a little drop in conductivity when aging was prolonged to 60 min. After that, however, prolonged aging (aging for 120 min) resulted in an increase in conductivity again. Similarly, in Fig. 9, increasing aging temperature led to a significant increase in conductivity, but a slightly lower conductivity value appeared at 510 °C. Figs. 8 and 9 reveal that a decrease in electrical conductivity occurred when the alloy was aged for 60 min at 510 °C, which is the condition corresponding to hardness peak. The phenomenon that a precipitation-hardenable alloy exhibits a rise in resistivity under the conditions nearly corresponding to the appearance of peak hardness is known as anomalous increase in resistivity.

From the electrical conductivity point of view, aging not only eliminates the defects, *e.g.*, excess vacancies and dislocations caused by quenching, but also reduces the amount of dissolved atoms in the matrix. On aging, a solution-treated alloy would obtain a continuous increase in its electrical conductivity, since the solute atoms come out of the matrix. However, not all precipitation-hardenable alloys can have a rise in conductivity under the condition nearly leading to the hardness peak. In addition to the present alloy, copper-beryllium alloys also show an anomalous increase in resistivity at maximum strength. When copper-beryllium alloys are age hardened to the highest strength, they have rather low conductivity of about 20 to 25% IACS (International Annealed Copper Standard).[9] This effect is probably caused by the scattering of electrons from the arrays of very fine precipitates, *e.g.*, Guinier-Preston zones, which result in maximum strength in most precipitation-hardenable alloys.[15]

3.3 Comparison with a Binary Cu-0.65 Wt.% Cr Alloy

One of the alloys studied in Ref 16 is a conventional Cu-Cr binary alloy containing about 0.65 wt.% Cr. It is interesting to compare this alloy with the present alloy. Undissolved particles in the Cu-0.65 wt.% Cr alloy are bcc Cr instead of bct Cr_3P. The maximum conductivity of aged Cu-0.65 wt.% Cr alloy is about 75% IACS, which is lower than that of the present alloy (90% IACS). The study in Ref 16 shows that undissolved Cr particles do not severely affect the electrical conductivity of Cu-0.65 wt.% Cr alloy. The high conductivity of Cu-0.6Cr-0.07P alloy also means that undissolved Cr_3P particles were not detrimental to the conductivity, probably because the formation of Cr_3P phase cleaned the matrix from the solute atoms.

The maximum hardness of Cu-0.65 wt.% Cr alloy is about HRB90 and it appears in the aging temperature range of 400 to 425 °C. In the present alloy, the peak hardness of about HV117 was obtained by aging in the temperature range from 480 to 510 °C. Aging below 450 °C could not yield the maximum hardness in Cu-0.6Cr-0.07P alloy. This difference between the two alloys may be due to the influence of phosphorus addition on alloy microstructures. The trace phosphorus or the chromium phosphide retards the growth of precipitates by locally depleting Cr through the formation of Cr_3P precipitates.[11] Furthermore, phosphorus atoms may segregate to the fcc/bcc interfaces to restrict their migration, thereby retarding the growth of precipitates. According to our present results, the competitive growth of Cr_3P phase particles during aging is another possible reason for the retarded growth of precipitates.

4. Conclusions

Undissolved particles in the solution-treated Cu-0.6Cr-0.07P alloy were identified as bct Cr_3P phase. They remained in as-aged structures, but increased in size during aging. The Cr_3P particles can impede dislocation motion, but their dispersion-strengthening effect is not strong due to their sparse distribution. The undissolved Cr_3P particles did not severely affect the electrical conductivity.

The presence of PFZ indicates that inhomogeneous precipitate nucleation occurs in the vicinity of grain boundaries in the later stages of aging. The precipitates grow from very fine and coherent agglomerates into coherent spherical particles in the course of aging. With a further increase in time and temperature, the precipitates coarsen into large rodlike particles so that they totally lose coherency with the matrix. Aging temperature influences properties and microstructures of the alloy more intensively than does aging time. The rodlike precipitates were identified as bcc Cr, but the formation of bct Cr_3P precipitates during overaging was not found in the present work.

The hardness increased with aging time and temperature and attained a maximum when the alloy was aged for 30 to 60 min at temperatures between 480 and 510 °C. Neither underaging nor overaging can result in the maximum hardness. The structure corresponding to the maximum hardness was characterized by a very fine and coherent precipitate morphology. Solution treating at 1000 °C is regarded as a good processing for Cu-0.6Cr-0.07P alloy.

The conductivity responds in a similar way to the hardness with increasing aging time and temperature, but a slight increase in resistivity was found near the same conditions producing peak hardness. As compared to a conventional Cu-0.65 wt.% alloy, Cu-0.6Cr-0.07P alloy needs a higher aging temperature to produce peak hardness, most probably because the phosphorus addition retards the growth of precipitates.

Acknowledgments

The authors thank Jussi Laurila for carrying out a part of the TEM work. Outokumpu Poricopper Oy provided the studied alloy. The research was funded by the Technology Development Center of Finland (TEKES).

References

1. R.O. Williams: *Trans. ASM*, 1960, vol. 52, pp. 530-38.
2. W. Koster and W Knorr: *Z. Metallkd.*, 1954, vol. 45, pp. 350-56.
3. J. Rezek: *Can. Met. Q.*, 1969, vol. 8, pp. 179-82.
4. R.W. Knights and P. Wilkes: *Metall. Trans.*, 1973, vol. 4, pp. 2389-93.
5. H. Suzuki and H. Kanno: *J. Jpn. Inst. Met.*, 1973, vol. 37, pp. 13-18.
6. J. Rys and Z. Rdzawski: *Met. Technol.*, 1980, vol. 7, pp. 32-35.

7. M.E. Drit, N.R. Bochvar, E.V. Lysova, and N.P. Leonova: *Sov. Non-Ferrous Met. Res.*, 1983, vol. 11 (4), pp. 312-16.
8. G.C. Weatherly, P. Humble, and D. Borland: *Acta Metall. Mater.*, 1979, vol. 27, pp. 1815-28.
9. *Metals Handbook*, 9th ed., vol. 4, *Heat Treating*, ASM International, Materials Park, OH, 1991, pp. 728-35.
10. M.J. Witcomb, U. Dahmen, and K.H. Westmacott: *Ultramicroscopy*, 1989, vol. 30, pp. 143-49.
11. C.P. Luo, U. Dahmen, M.J. Witcomb, and K.H. Westmacott: *Scripta Metall. Mater.*, 1992, vol. 26, pp. 649-54.
12. M.F. Ashby and L.M. Brown: *Phil. Mag.*, 1963, vol. 8, pp. 1083-103.
13. D.A. Porter and K.E. Easterling: *Phase Transformations in Metals and Alloys*, Van Nostrand Reinhold Company Ltd., Berkshire, United Kingdom, 1981, pp. 303-05 and 314-17.
14. T. Gladman: *Mater. Sci. Technol.*, 1999, vol. 15 (1), pp. 30-36.
15. P. L. Rossiter: *The Electrical Resistivity of Metals and Alloys*, Cambridge University Press, Cambridge, United Kingdom, 1991, p. 258.
16. C.J. Kim and J.M. Lee: *J. Mater. Proc. Man. Sci.*, 1994, vol. 2 (1), pp. 325-34.